PCCP

PAPER

View Article Online
View Journal | View Issue

Cite this: *Phys. Chem. Chem. Phys.*, 2017, **19**, 28037

A novel explanation for the enhanced colloidal stability of silver nanoparticles in the presence of an oppositely charged surfactant†

Sara Skoglund, ‡*[a] Eva Blomberg, *[ab] Inger Odnevall Wallinder, [a] Isabelle Grillo, [c] Jan Skov Pedersen [d] and L. Magnus Bergström §*[a]

Received 11th July 2017,
Accepted 3rd October 2017

DOI: 10.1039/c7cp04662f

rsc.li/pccp

The structural behavior in aqueous mixtures of negatively charged silver nanoparticles (Ag NPs) together with the cationic surfactants cetyltrimethylammonium bromide (CTAB) and dodecyltrimethylammonium chloride (DTAC), respectively, has been investigated using SANS and SAXS. From our SANS data analysis we are able to conclude that the surfactants self-assemble into micellar clusters surrounding the Ag NPs. We are able to quantify our results by means of fitting experimental SANS data with a model based on cluster formation of micelles with very good agreement. Based on our experimental results, we propose a novel mechanism for the stabilization of negatively charged Ag NPs in a solution of positively charged surfactants in which cluster formation of micelles in the vicinity of the particles prevents the particles from aggregating. Complementary SAXS and DLS measurements further support this novel way of explaining stabilization of small hydrophilic nanoparticles in surfactant-containing solutions.

Introduction

Surfactants are often used to stabilize nanoparticles (NPs) in solution.[1–7] Nanoparticles and surfactants also frequently come into contact in many applications. Silver nanoparticles (Ag NPs), which are often incorporated in sports clothing, can be released during the laundry cycle and interact with surfactants in the washing powder.[8–11] Surface interactions between Ag NPs and surfactants influence their stability in solution. This may further influence their subsequent transport *via* different chemical transients, and influence their bioavailability and toxicity.[10,12–14] A better understanding of these interactions is consequently of high importance to enable predictions of the fate of Ag NPs released from *e.g.* consumer products. The stability of released Ag NPs during a laundry cycle has previously been investigated with a number of different techniques, notably zeta potential, dynamic light scattering (DLS), atomic absorption spectroscopy (AAS), quartz crystal microbalance with dissipation (QCM-D) and Raman spectroscopy.[11,15,16] The stability of the Ag NPs was in these studies shown to depend on the charge and concentration of the interacting surfactants. The Raman spectroscopy measurements did not indicate any chemical bonding between the Ag NPs and the surfactants.[15] One of the surfactants that were investigated in these studies is dodecyltrimethylammonium chloride (DTAC), which is a cationic surfactant. At low DTAC concentrations, interactions with negatively charged Ag NPs resulted in charge neutralization and formation of large structures. Eventually, the surface charge of the Ag NPs changed sign to positive values as the DTAC concentration was further increased. This behavior was suggested to be a result of a patchy bilayer formation of DTAC on the Ag NPs that prevents agglomeration due to repulsive electrostatic forces between the positively charged colloidal particles.[11,15,17] Similarly, in a recent small-angle neutron scattering (SANS) study on gold nanorods in cetyltrimethyl-ammonium bromide (CTAB), the surfactants were proposed to be present in a bilayer structure at the nanorod interface.[18] Other studies suggest that the surfactant molecules stabilize NPs by forming a bilayer-like assembly surrounding the NPs.[4]

Lugo *et al.*[19] have studied the adsorption of the nonionic surfactant pentaethylene glycol monododecyl ether ($C_{12}E_5$) on hydrophobic silica NPs in an aqueous solvent with contrast matching SANS. From the characteristic scattering behavior the

[a] *KTH Royal Institute of Technology, School of Chemical Science and Engineering, Surface and Corrosion Science, SE-100 44 Stockholm, Sweden. E-mail: blev@kth.se, Magnus.Bergstrom@farmaci.uu.se, sarasko@kth.se*
[b] *RISE Research Institutes of Sweden, Division Bioscience and Materials, Stockholm, Sweden*
[c] *Institut Laue Langevin, DS/LSS, Grenoble, France*
[d] *Department of Chemistry and Interdisciplinary Nanoscience Center (iNANO), Aarhus University, Aarhus, Denmark*

† Electronic supplementary information (ESI) available: Details on the least-square model fitting SANS data analysis and results, in form of SANS curves offset and a table with the fitting parameters. See DOI: 10.1039/c7cp04662f

‡ Present address: Department of Materials and Environmental Chemistry Arrhenius Laboratory, Stockholm University, Stockholm, Sweden.
§ Present address: Department of Pharmacy, Uppsala University, Uppsala, Sweden.

authors were able to conclude that hemi-micellar patches of the surfactant were adsorbed onto the silica particles. This behavior may be rationalized as a result of the hydrophobic effect and the tendency of the hydrophobic surfactant tails and the silica particle interfaces to avoid solvent water. The formation of micelles on the particles was also suggested in a study on dimethyldodecylamine-*N*-oxide C_{12}DAO and silica NPs of various size.[20]

In the present paper we investigate the self-assembly of the cationic surfactant CTAB in presence of negatively charged Ag NPs. Since Ag NPs are more hydrophilic than, for instance, silica particles and the surfactant molecules, they are not likely to adsorb directly onto the particles as a result of the hydrophobic effect. CTAB resembles DTAC but with a longer hydrocarbon chain and lower critical micelle concentration (CMC). The CMC for DTAC is 20 mM and approximately 1 mM for CTAB at 30 °C.[10] We have chosen to primarily study mixtures of CTAB and Ag NPs since the self-assembly behavior of CTAB is well known from SANS measurements. CTAB forms small non-spherical ellipsoidal micelles (half-axes $a \approx 2$ nm, $b \approx 3$ nm and $c \approx 4$ nm) in pure water.[21] Previous attempts to determine the structure of self-assembled surfactants on other hard matter–soft matter interfaces with cryo-TEM and other electron microscopy techniques have not been successful.[22–24] The most powerful approach to find out the structure of self-assembled surfactants in the vicinity of Ag NPs is probably to combine SANS and small angle X-ray scattering (SAXS). SAXS predominantly provides information of silver in the Ag NPs, whereas SANS provides information of the surfactant made up of hydrogen in a deuterium oxide solvent.[25,26] Below we propose a novel mechanism, based on the structural behavior as determined with a combination of SANS and SAXS, for the stabilization of negatively charged Ag NPs in the presence of the positively charged surfactants CTAB and DTAC, respectively.

Experimental

Materials

Sodium borohydride ($NaHB_4$), deuterium dioxide (D_2O), silver nitrate ($AgNO_3$), cetyltrimethylammonium bromide (CTAB), and dodecyltrimethylammonium chloride (DTAC), were all purchased from Sigma Aldrich (reagent grade) and used without further purification.

Sample preparation

All solutions were prepared in D_2O and all glassware were prior to the synthesis cleaned with 10% HNO_3 for 24 h followed by Hellmanex® for 24 h. The Ag NPs were synthesized based on a procedure developed by Creighton *et al.*[27] 25 mL of a 10 mM $AgNO_3$ solution was added drop-wise to a 25 mL ice-cooled 30 mM $NaBH_4$ solution under vigorous stirring. The solution was stored under dark conditions for a couple of days prior to use in order to allow borohydride decomposition. The final Ag concentration (300 ± 10 mg L^{-1}) in solution (*i.e.* non-sedimented particles and complexes) directly after preparation was determined by means of atomic absorption spectroscopy (AAS). The used buffer concentrations differed somewhat from the recipe of Creighton *et al.*[19] since the concentrations in the present study were optimized with respect to the concentrations of Ag NPs and the surfactant needed to obtain a high enough signal in the SANS experiments, and to a concentration at which the Ag NPs remained stable in solution with the surfactants for at least 1 month. The stability of the particles was verified by means of dynamic light scattering (DLS) using an instrument employing photon cross correlation spectroscopy (PCCS). A stock solution of the CTAB or DTAC (10 wt%) was prepared and added drop-wise to the Ag NPs solution, followed by gentle shaking of the test tubes. The solutions were prepared 48 h prior to the SANS measurements and 2 weeks prior to the SAXS experiments. The stability of these dispersions during these time periods was verified by means of PCCS for solutions containing both Ag NPs and surfactants, and solutions with Ag NPs only. Within this time period the Ag NPs without surfactants formed agglomerates and sedimented to a large extent (scattered light intensities decreased from approx. 1300 kcps to 20 kcps). All experiments were performed at 30 °C to avoid precipitation of CTAB (the Krafft temperature of CTAB and DTAC in D_2O is 29 °C and 23 °C, respectively).

Photon cross correlation spectroscopy (PCCS)

PCCS measurements were performed using a NanoPhox instrument (Sympatec, Germany). Single samples were measured three times each at 30 °C. Data from the unique measurements was integrated to produce a single distribution with the PCCS software (Windox 5). The samples were measured 24 h after preparation as well as 1 month later. Standard latex samples (20 ± 2 nm) (Sympatec) and blank samples were analyzed prior to the measurements to ensure a high accuracy of the measurements.

Atomic absorption spectroscopy (AAS)

Determination of the Ag concentration in solution was performed by means of AAS (Perkin-Elmer AAnalyst 800) using a graphite furnace accessory. Calibration standards of 0, 7.5, 15, 30, and 45 μg Ag L^{-1} were prepared from a 1 g L^{-1} standard (PerkinElmer). Prior to analysis, the non-sedimented fraction of the samples was digested (2.5 mL sample, 1 mL 30 wt% H_2O_2, 100 μL 30 wt% HCl and 6.4 mL Milli-Q water) *via* UV treatment (Metrohm 705 UV digester, 500 W, 95 °C for 2 h) to ensure analysis of the total amount of Ag in solution. The detection limit was estimated to 10 μg L^{-1} in the surfactant solution based on the *t*-value for a 99% confidence interval (3.49, $n = 6$) multiplied by the standard deviation of blank values.[28] Triplicate readings were analyzed for each sample and control samples of known Ag concentration were analyzed in parallel, showing acceptable recoveries of added amounts (85–100%). Blank and standard samples were measured throughout the analysis and all samples were diluted to fall within the calibration range (10–45 μg L^{-1}).

Zeta potential

The ζ-potential of the pure Ag NPs (-44 ± 5 mV) in Milli-Q water was determined by means of laser Doppler microelectrophoresis

using a Zetasizer Nano ZS instrument (Malvern Instruments, UK) at 25 °C based on three replica samples measured twice per sample. This potential is in line with previous findings.[15,29]

Small-angle neutron scattering (SANS)

SANS experiments were carried out at the D11 SANS instrument at Institute Laue-Langevin (ILL), Grenoble, France. A range of scattering vectors, q, from 0.003 to 0.5 Å^{-1}, was covered by three sample-to-detector distances (d = 1.2, 8, and 20 m) at the neutron wavelength λ of 6.0 Å. The settings (d = 8 m, λ = 6.0 Å) and (d = 20 m, λ = 6.0 Å), respectively, were used as reference settings for the absolute scale. The wavelength resolution was 10% (full width at half-maximum value). The samples were kept in quartz cells (Hellma) with path lengths of 1 or 2 mm. The selected path length depended on the surfactant concentration, and thus the scattering intensity in the sample. SANS data was analysed with a model for ellipsoidal micelles that form clusters in the vicinity of the Ag NPs. The model is based on the Baxter sticky hard-sphere model.[30] More details are given in the ESI.†

Small-angle X-ray scattering (SAXS)

Data was collected on the SAXS pinhole camera at Aarhus University, Denmark,[31] equipped with a rotating anode giving CuKα radiation with a wavelength of λ = 1.54 Å. For the measurements, the instrument was set up with a long sample detector distance (106 cm) and small pinholes to cover the range of scattering vectors 0.004–0.22 Å^{-1}. The pinhole before the sample was a custom-made scatterless square.[32] The samples were measured in a custom-made flow-through quartz capillary, and background scattering from pure buffer solutions was subtracted from the sample scattering. Generated SAXS data for the Ag NPs was modelled using a model with polydisperse spheres with a Gaussian number size distribution[26] and a fractal structure factor for describing their clustering.[33] The difference in scattering length density between Ag NP and solvent D_2O was estimated to $\Delta\rho = -2.9 \times 10^{10}$ cm^{-2} and for CTAB and DTAC to $\Delta\rho = -66.4$ cm^{-2} and $\Delta\rho = -63.8$ cm^{-2} respectively.

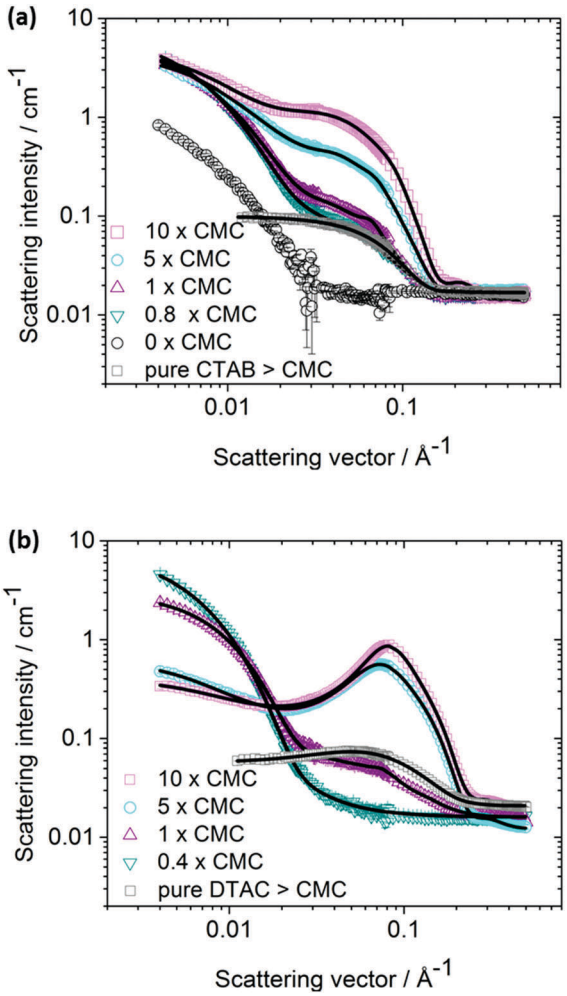

Fig. 1 SANS scattering intensity as a function of the scattering vector q for mixtures of Ag NPs (300 mg L^{-1}) and CTAB (a) or DTAC (b), of varying surfactant concentration (10 × CMC (□), 5 × CMC (○), 1 × CMC (△) and 0.8 × CMC (in a) or 0.4 × CMC (in b) (▽)), as well as for a solution of 2 × CMC pure surfactant only (□). In (a) also the Ag NPs only (○) are shown. The symbols represent SANS data, and the solid lines represent the best fits with a model for micelle clusters present in the vicinity of the particles.

Results and discussion

Small-angle neutron scattering (SANS)

SANS data for several Ag NP–CTAB mixtures with different surfactant concentrations, as well as for samples of Ag NPs only and CTAB only, is shown in Fig. 1a. As expected, the scattering contrast of silver was found to be very weak in D_2O as compared to hydrogen in the surfactant, in particular at higher q-values. As a result, it is predominantly the self-assembled CTAB that contributes to the scattering behavior of samples containing surfactant observed in Fig. 1a. Notably, it is seen that the scattering intensities observed at low q-values for all samples that contain both Ag NPs and surfactant are much higher than for the corresponding data of either pure Ag NPs or pure surfactant. The contribution from the comparatively small repelling CTAB micelles to the scattered intensity below approximately 0.01 Å^{-1} is expected to be small.[34] Hence, we may conclude that the presence of Ag NPs has a significant influence on the structural behavior of the surfactant and that the observed high intensities at low q-values must originate from some larger structures formed by the surfactant. Corresponding results for the Ag NP–DTAC system are shown in Fig. 1b. We have in a previous paper speculated that the stabilization effect between Ag NPs and surfactants such as CTAB and DTAC derives from a bilayer type of positively charged formation on the particles[11] as schematically illustrated in Fig. 2a. However, such a model is not consistent with the SANS data of this study that lacks the typical feature of a bilayer structure or micelles adsorbed to the particle surface [*cf.* Fig. 1]. A bilayer shell,[35] as well as micellar patches[19,20] adsorbed onto the particles would give rise to a typical oscillating pattern that cannot be seen in our SANS data, and no indications at all imply that the surfactant is directly adsorbed onto the Ag NPs. The assumption that the surfactants form micellar clusters in the vicinity of the charged particles, schematically illustrated

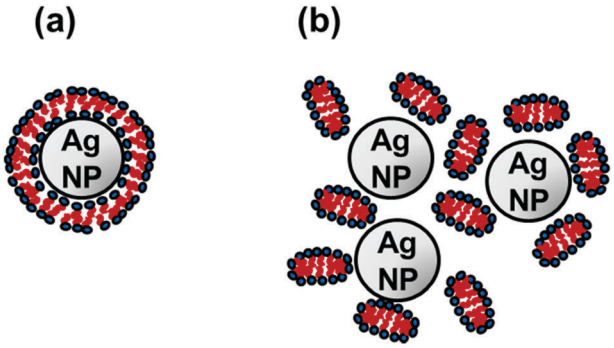

Fig. 2 Schematic representation of two possible mechanisms of the stabilization of Ag NPs by surfactants; (a) the bilayer type formation on the particles, and (b) the micelle cluster formation in the vicinity of the particles. Only the latter model is consistent with our SANS data.

in Fig. 2b, agrees excellently with our SANS data. In particular, the proposed model of micellar clusters forming in the vicinity of the NPs, as shown in Fig. 2b, accounts for the high scattering intensities at low q-values as well as the micellar-like behaviour observed at approximately $q = 0.05$ Å^{-1} [*cf.* further below].

These clusters may form already well below CMC of pure CTAB or DTAC due to higher local concentration of surfactant close to the Ag NP surface. Notably, Fig. 2 is merely a schematic illustration. In reality, the particles are probably polydisperse and not strictly spherical in shape [*cf.* Fig. 3b].

In contrast to the case of hydrophobic NPs, there is no driving force due to the hydrophobic effect that facilitates the formation of a monolayer or hemi-micelles on hydrophilic Ag NPs below CMC. The formation of a bilayer is not expected by a micelle forming ionic surfactant with a comparatively high spontaneous curvature.[21] Moreover, since surfactant head groups as well as Ag NPs are mainly hydrophilic, they prefer to be located adjacent to water molecules rather than the surfactants being directly physisorbed onto the Ag NPs. On the other hand, there is a considerable entropy gain for the charged Ag NPs to exchange a large number of small counter-ions with much fewer large multivalent CTAB micelles. Similarly, the Br^- counter-ions of the CTAB micelles are simultaneously exchanged with negatively charged Ag NP macro-ions implying that oppositely charged multivalent micelles and NPs tend to form larger cluster-like structures, in accordance with our observations with SANS. Hence, the Ag NP may be considered as a negatively charged giant multivalent counter-ion to the self-assembled positively charged cationic surfactant CTA^+. The mechanism is analogous to the exchange of counter-ions of colloidal particles to ions with higher charge numbers. A similar mechanism of association has also been suggested for the formation of large complexes formed in aqueous mixtures of oppositely charged polyelectrolytes. The formation of structures larger than single surfactants was observed with SANS far below the CMC of the surfactant only. This indicates that the surfactants are affected by the presence of the Ag NPs and that micellar aggregates are formed already at concentrations well below the CMC (20 mM for DTAC and 1.0 mM for CTAB[10]). Objects much larger than single surfactants could be observed in solutions with concentrations

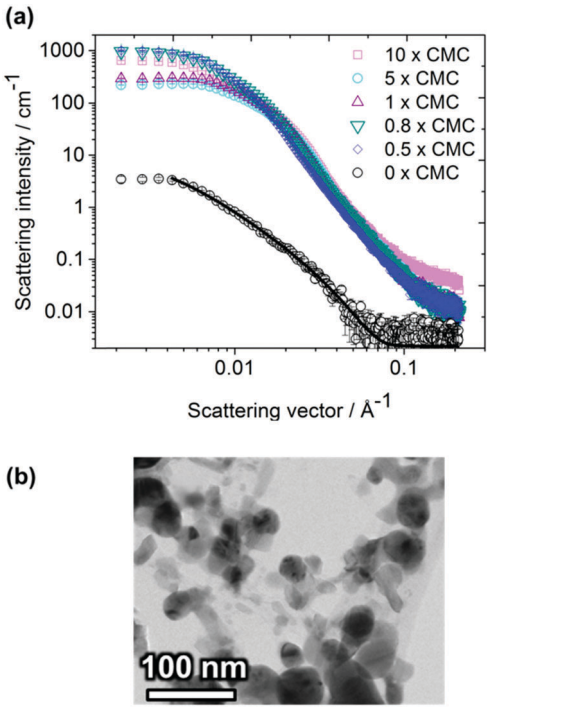

Fig. 3 (a) SAXS cross section as a function of the scattering vector q for mixtures of Ag NPs and CTAB of varying surfactant concentration (10 × CMC (□), 5 × CMC (○), 1 × CMC (△), 0.8 × CMC (▽) and 0.5 × CMC (◊)) as well as for a solution of Ag NPs only (○). The initial concentration of Ag NPs was 300 mg L^{-1}. The symbols represent SAXS data, and the solid line for Ag NPs only represents the best fit obtained with a fractal model of polydisperse spheres. (b) Bright field TEM image of the Ag NPs (prepared from a particle suspension of 25 mg L^{-1} without surfactant bath sonicated for 1 min and dried on holey carbon coated copper grids). EDS analysis confirmed their silver content.

corresponding to half the CMC of the pure surfactant. In accordance, the SANS data shown in Fig. S1, S2 (ESI†) and Fig. 1, displays the characteristic scattering behaviour of surfactant micelles at approximately 0.1 Å^{-1}, also at concentrations well below the CMC of the pure surfactant. The SANS data obtained from a sample containing only Ag NPs without any surfactant, lacks this typical feature of micelles. Moreover, the scattering intensity monitored for this particular sample was significantly smaller than for solutions including the surfactant.

Model fitting analysis

In order to further test the validity of our proposed cluster model, we have carried out a quantitative least-square model fitting analysis of the SANS data. The model is described in detail in the ESI.† Examples of model fits are included in Fig. 1 and the excellent agreement between model and observed data is apparent. The very same data is also shown in Fig. S2 (ESI†) with an offset for each surfactant concentration in order to better elucidate individual curves. Obtained results of the fitting parameters are given in Table S1 (ESI†). The cluster formation of micelles is taken into account by a structure factor derived in accordance with a sticky hard sphere model.[30] This model corresponds to hard spheres with surface adhesion and has,

for instance, previously been used to describe the structure of sterically stabilized silica colloidal particles.[35,36] The attractive force assembling the positively charged micelles that surround the Ag NPs originates from the oppositely charged Ag NPs that scatter more weakly and its contribution to the SANS data is therefore negligible. In addition to attraction between micelles and NPs, repulsion due to double layer forces that take place between the positively charged micelles is taken into account in the model. The model also takes into account the fact that only a fraction of the micelles is associated to the NPs and that a large fraction of the micelles are non-associated in solution. At surfactant concentrations exceeding the CMC, the fraction of associated micelles is evidently much smaller than below CMC.

This observation agrees very well with our proposed model where a certain number of micelles are loosely associated to the Ag NPs. The increase in number of micelles with increasing surfactant concentration is clearly seen from the SANS data in Fig. 1 as an increase in intensity at about $q = 0.04$ Å^{-1} and 0.1 Å^{-1} for CTAB and DTAC respectively. The fact that the model applies above, as well as below the CMC for pure CTAB further supports our proposed mechanism. The presence of CTAB micelles close to the NP surface, rather than CTAB being chemically bonded to the silver surface, is further supported by our recent Raman spectroscopy studies on a similar system.[15] The observed reduction of the CMC of CTAB as oppositely charged NPs are present may be rationalized as the result of an increase in entropy as the conventional Br^- counter-ions of micelles are released and exchanged with Ag NPs. As a consequence, the chemical potential of CTAB is reduced and so is CMC. In addition, the solutions may also contain a small amount of residual electrolyte components, resting from the synthesis, which could further slightly reduce the CMC. Moreover, as Ag^+ will be released from the NPs, the ionic strength of the solution will potentially increase,[14,37] thus lowering the CMC. Oxidative etching of the Ag NPs might furthermore be increased by the Br^- counter-ions in the solution, and AgBr will most likely form.[38] However, all these latter effects are likely to be of minor importance in comparison with the main association mechanism. SANS data on DTAC–Ag NPs is presented in Fig. 1b together with fitting results using the identical model, and also in this case the agreement between model and data is excellent.

Small-angle X-ray scattering (SAXS)

The same samples of Ag NPs and surfactants in D_2O that were investigated with SANS were also investigated with SAXS (*cf.* Fig. 3 for CTAB and Fig. S3 (ESI†) for DTAC). Since the excess electron density of silver is much larger than for the common elements in the surfactant, the SAXS data is completely dominated by the contribution from the Ag NPs. Since the samples containing Ag NPs are non-stable, and particles sedimented from the solution, the intensity was found to be considerably lower than for samples with both Ag NPs and surfactant. Data for the Ag NPs could be fitted with a fractal model of polydisperse spheres.[33] The NPs were found to be rather small, with a number-average radius equal to 4.1 ± 0.3 nm for a fractal dimension of 2.21 ± 0.06 and a cluster radius of gyration of 50 nm.

Notably, the intensity in the low-q regime is seen to decrease with increasing surfactant concentration (except at 10 × CMC where the surfactant apparently contributes to the SAXS data). This is indicative of an increased repulsion between the Ag NPs as the amount of surfactant added increase. According to the conventional model for the stability of charged colloidal particles, an entropic repulsive force due to the overlapping diffuse layers of counter-ions prevents the colloidal NPs from aggregating. Most interestingly, the model based on the SANS data, *i.e.* clusters of micelles that form in the proximity of the Ag NPs, suggests a strongly enhanced repulsive stabilizing effect of the NPs. In addition to Ag NPs, the CTAB micelles are surrounded by a diffuse repulsive layer of Br^- counter-ions. Similarly, the Ag NPs are surrounded by a diffuse layer of micelle clusters that is expected to contribute with an additional repulsive effect. As a result, we expect the diffuse layers of counter-ions, as well as from micelles in clusters, to overlap when two Ag NPs approach one another, causing an enhanced repulsion that stabilizes the dispersion.

The strong repulsion observed with SAXS means that the true diameter of the Ag NP clusters is probably somewhat larger than what the SAXS results indicate. The 10 × CMC sample does not follow the same trend, which indicates that the surfactant

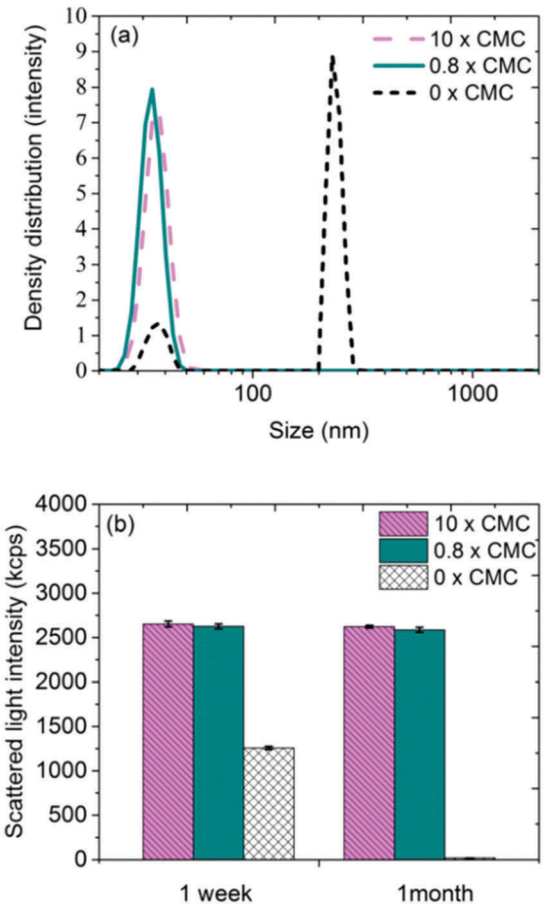

Fig. 4 (a) Particle size distributions based on intensity density of Ag NPs in different concentrations of CTAB, 1 week after preparation, and (b) corresponding scattered light intensities after 1 week and 1 month after preparation.

may contribute significantly to the scattered intensity at very high surfactant concentrations. Samples containing Ag NPs only, without any surfactant, scattered considerably less as compared with samples containing both Ag NPs and surfactant. The reason is probably that the Ag NPs start to agglomerate almost immediately in the absence of a stabilizing surfactant and sediment from the solution.[39] This is confirmed by colloidal stability measurements of Ag NPs by means of PCCS. Intensity size distributions one week after preparation are shown in Fig. 4a for Ag NPs in CTAB solutions above (10 × CMC) and below CMC (0.8 × CMC), as well as in Ag NP-solutions without surfactant.

The difference between the samples with and without surfactant is conspicuous, where the latter, in addition to structures sized approximately 30 nm, shows sizes of several 100 nm. This peak originates from the formation of larger structures in the absence of stabilizing surfactant. After one month, similar size distributions as observed after one week were evident for the samples containing surfactant [*cf.* Fig. 4b]. Samples without surfactant did not give rise to any measurable signals due to fast sedimentation of particles from solution.

A likely explanation is that the 30–50 nm structures observed using PCCS and SAXS consist of a number of clustered Ag NPs, each approximately sized 8 nm (as determined with SAXS) as illustrated in Fig. 2b. The considerably small size of the Ag NPs seems to better agree with the micellar cluster hypothesis than with the assumption that largely curved bilayers form on the top of the highly curved Ag NPs [*cf.* Fig. 2].

SAXS and PCCS data for Ag NPs–DTAC, shown in Fig. S3 and S4 in the ESI,† appear similar to the corresponding data for Ag NP–CTAB.

Conclusions

SANS and SAXS measurements have been combined to investigate the structure and mechanism for particle stabilization in aqueous mixtures of negatively charged silver nanoparticles (Ag NPs) and the cationic surfactants cetyltrimethylammonium bromide (CTAB) and dodecyltrimethylammonium chloride (DTAC). The following main conclusions are drawn:

- Complementary SANS and SAXS measurements are proven able to provide in-depth knowledge of the interaction between anionic Ag NPs and the cationic surfactants CTAB and DTAC.
- The SANS data is consistent with the formation of micellar clusters surrounding the Ag NPs. The clusters form well below the critical micelle concentration of the pure surfactant. However, there is no support of any kind in our SANS data that the surfactant adsorbs directly onto the Ag NPs.
- By applying a sticky hard-sphere model, which takes into account cluster formation of micelles, robust and reliable least-square model fits of SANS data could be carried out. These findings are supported by SAXS and PCCS observations of the same samples.
- A novel way of explaining the stabilization of small and fairly hydrophilic NPs in solutions containing oppositely charged surfactant is proposed, where the mechanism behind the stabilization of negatively charged Ag NPs by the cationic surfactants CTAB and DTAC is governed by the formation of micelle clusters in the close vicinity of the NPs.

Conflicts of interest

There are no conflicts to declare.

Acknowledgements

The authors highly appreciate the ILL facility for the allocated beam-time at the D11 SANS-instrument for proposal 9-12-365. The authors are grateful to Dr M. Tornberg at Swerea KIMAB for assistance with the TEM measurements. We also thank Prof. M. Toprak and Dr J. Hedberg at KTH Royal institute of Technology and Dr M. Lundin Johnson and Dr A. Sugunan at SP Technical Research Institute of Sweden, for valuable discussions regarding the particle synthesis. The Swedish Research Council (grant no. 2013-5621) is acknowledged for financial support.

References

1 C. Marambio-Jones and E. Hoek, *J. Nanopart. Res.*, 2010, **12**, 1531–1551.
2 A. El Badawy, T. Luxton, R. Silva, K. Scheckel, M. Suidan and T. Tolaymat, *Environ. Sci. Technol.*, 2010, **44**, 1260–1266.
3 Z. Sui, X. Chen, L. Wang, L. Xu, W. Zhuang, Y. Chai and C. Yang, *Physica E*, 2006, **33**, 308–314.
4 S. Majumder, B. Naskar, S. Ghosh, C.-H. Lee, C.-H. Chang, S. P. Moulik and A. K. Panda, *Colloids Surf., A*, 2014, **443**, 156–163.
5 M. Chakraborty, F.-W. Hsiao, B. Naskar, C.-H. Chang and A. K. Panda, *Langmuir*, 2012, **28**, 7282–7290.
6 S. Moulik, G. De, A. Panda, B. Bhowmik and A. Das, *Langmuir*, 1999, **15**, 8361–8367.
7 A. Panda, S. Moulik, B. Bhowmik and A. Das, *J. Colloid Interface Sci.*, 2001, **235**, 218–226.
8 L. Geranio, M. Heuberger and B. Nowack, *Environ. Sci. Technol.*, 2009, **43**, 8113–8118.
9 T. Benn and P. Westerhoff, *Environ. Sci. Technol.*, 2008, **42**, 4133–4139.
10 E. Smulders, W. Rybinski, E. Sung, W. Rähse, J. Steber and A. Nordskog, *Laundry Detergents*, Wiley Online Library, Weinheim, 2007.
11 S. Skoglund, T. A. Lowe, J. Hedberg, E. Blomberg, I. Odnevall Wallinder, S. Wold and M. Lundin, *Langmuir*, 2013, **29**, 8882–8891.
12 L. Kvitek, A. Panacek, J. Soukupova, M. Kolar, R. Vecerova, R. Prucek, M. Holecova and R. Zboril, *J. Phys. Chem. C*, 2008, **112**, 5825–5834.
13 E. Bae, H.-J. Park, J. Park, J. Yoon, Y. Kim, K. Choi and J. Yi, *Bull. Korean Chem. Soc.*, 2011, **32**, 613–619.
14 J. Liu, D. Sonshine, S. Shervani and R. Hurt, *ACS Nano*, 2010, **4**, 6903–6913.

15 J. Hedberg, M. Lundin, T. Lowe, E. Blomberg, S. Wold and I. Odnevall Wallinder, *J. Colloid Interface Sci.*, 2012, **369**, 193–201.
16 J. Hedberg, S. Skoglund, M.-E. Karlsson, S. Wold, I. Odnevall Wallinder and Y. Hedberg, *Environ. Sci. Technol.*, 2014, **48**, 7314–7322.
17 Z. M. Sui, X. Chen, L. Y. Wang, Y. C. Chai, C. J. Yang and J. K. Zhao, *Chem. Lett.*, 2005, **34**, 100–101.
18 S. Gomez-Grana, F. Hubert, F. Testard, A. Guerrero-Martinez, I. Grillo, L. Liz-Marzan and O. Spalla, *Langmuir*, 2012, **28**, 1453–1459.
19 D. Lugo, J. Oberdisse, M. Karg, R. Schweins and G. Findenegg, *Soft Matter*, 2009, **5**, 2928–2936.
20 D. M. Lugo, J. Oberdisse, A. Lapp and G. H. Findenegg, *J. Phys. Chem. B*, 2010, **114**, 4183–4191.
21 L. M. Bergström and I. Grillo, *Soft Matter*, 2014, **10**, 9362–9372.
22 A. Neyman, L. Meshi, L. Zeiri and I. Weinstock, *J. Am. Chem. Soc.*, 2008, **130**, 16480–16481.
23 C. Ophus, J. Ciston, J. Pierce, T. Harvey, J. Chess, B. McMorran, C. Czarnik, H. Rose and P. Ercius, *Nat. Commun.*, 2016, **7**, 1–7.
24 Z. Lee, K. Jeon, A. Dato, R. Erni, T. Richardson, M. Frenklach and V. Radmilovic, *Nano Lett.*, 2009, **9**, 3365–3369.
25 P. Lindner and T. Zemb, Neutron, X-ray and light scattering: introduction to an investigative tool for colloidal and polymeric systems: proceedings of the European Workshop on Neutron, X-Ray and Light Scattering as an Investigative Tool for Colloidal and Polymeric Systems, Bombannes, France, 27 May–2 June, 1990, North-Holland, Amsterdam, 1991.
26 J. S. Pedersen, *Adv. Colloid Interface Sci.*, 1997, **70**, 171–210.
27 J. A. Creighton, C. G. Blatchford and M. G. Albrecht, *J. Chem. Soc., Faraday Trans.*, 1979, **2**, 790–798.
28 J. T. Creed, T. D. Martin, L. B. Lobring and J. W. O'Dell, *Environmental Monitoring Systems Laboratory Office of Research and Development*, 1994, pp. 1–42.
29 R. A. Alvarez-Puebla, E. Arceo, P. J. G. Goulet, J. J. Garrido and R. F. Aroca, *J. Phys. Chem. B*, 2005, **109**, 3787–3792.
30 R. J. Baxter, *J. Chem. Phys.*, 1968, **49**, 2770–2774.
31 J. S. Pedersen, *J. Appl. Crystallogr.*, 2004, **37**, 369–380.
32 Y. Li, R. Beck, T. Huang, M. Choi and M. Divinagracia, *J. Appl. Crystallogr.*, 2008, **41**, 1134–1139.
33 J. Teixeira, *J. Appl. Crystallogr.*, 1988, **21**, 781–785.
34 G. Fleer, M. Cohen Stuart, J. Scheutjens, T. Cosgrove and B. Vincent, *Polymers at Interfaces*, Chapman and Hall, London, 1995.
35 M. Duits, R. May, A. Vrij and C. G. De Kruif, *J. Chem. Phys.*, 1991, **94**, 4521–4531.
36 C. G. De Kruif and J. C. Van Miltenburg, *J. Chem. Phys.*, 1990, **93**, 6865–6869.
37 J. Y. Liu and R. H. Hurt, *Environ. Sci. Technol.*, 2010, **44**, 2169–2175.
38 F. Wu, W. Wang, Z. Xu and F. Li, *Sci. Rep.*, 2015, **5**, 1–7.
39 H. van Olphen, *An introduction to clay colloid chemistry*, Wiley Subscription Services, Inc., A Wiley Company, New York, 1964.